Acta Cryst. (1993). D**49**, 362-365

2.2 Å Refined Crystal Structure of the Catalytic Subunit of cAMP-Dependent Protein Kinase Complexed with MnATP and a Peptide Inhibitor

BY JIANHUA ZHENG [1], ELZBIETA A. TRAFNY [2], DANIEL R. KNIGHTON [1],* NGUYEN-HUU XUONG [1,3,4], SUSAN S. TAYLOR [1], LYNN F. TEN EYCK [1,5] AND JANUSZ M. SOWADSKI [2]†

[1] *Department of Chemistry, University of California, San Diego,* 9500 *Gilman Drive, La Jolla, CA* 92093-0654, *USA*

[2] *Department of Medicine, University of California, San Diego,* 9500 *Gilman Drive, La Jolla, CA* 92093-0654, *USA*

[3] *Department of Biology, University of California, San Diego,* 9500 *Gilman Drive, La Jolla, CA* 92093-0317, *USA*

[4] *Department of Physics, University of California, San Diego,* 9500 *Gilman Drive, La Jolla, CA* 92093-0317, *USA*

[5] *San Diego Supercomputer Center, PO Box* 85608, *San Diego, CA* 92186-9784, *USA*

(*Received* 15 *December* 1992; *accepted* 12 *January* 1993)

Abstract. The crystal structure of a ternary complex containing the catalytic subunit of cAMP-dependent protein kinase, ATP and a 20-residue inhibitor peptide was refined at a resolution of 2.2 Å to an *R* value of 0.177. In order to identify the metal binding sites, the crystals, originally grown in the presence of low concentrations of Mg^{2+}, were soaked in Mn^{2+}. Two Mn^{2+} ions were identified using an anomalous Fourier map. One Mn^{2+} ion bridges the γ- and β-phosphates and interacts with Asp184 and two water molecules. The second Mn^{2+} ion interacts with the side chains of Asn171 and Asp184 as well as with a water molecule. Modeling a serine into the P site of the inhibitor peptide suggests a mechanism for phosphotransfer.

Introduction. Protein kinases constitute a large and diverse family of enzymes (Hanks, Quinn & Hunter, 1988). One member of this family is the catalytic (*C*) subunit of cyclic 3′,5′-adenosine monophosphate (cAMP)-dependent protein kinase (cAPK). The crystal structure of the mouse recombinant C_α subunit was solved to a resolution of 2.7 Å (Knighton *et al.*, 1991). A mutant form (Ser139Ala) of this enzyme was recently refined further to 2.0 Å resolution (Knighton *et al.*, 1993). These structures are binary complexes containing the *C* subunit and a high affinity 20-residue inhibitor peptide derived from the amino-terminal portion of a naturally occurring heat-stable protein-kinase inhibitor (PKI). However, in order to understand more fully the functioning of this enzyme, the structure of a ternary complex containing the *C* subunit, an inhibitor peptide [PKI(5-24)] and MgATP was recently solved to 2.7 Å resolution (Zheng *et al.*, 1993). This structure defines the orientation of the nucleotide and the interactions of MgATP with numerous conserved residues at the active site.

The nucleotide binds primarily to the small lobe with the base occupying a sterically constrained hydrophobic pocket. The non-transferable α- and β-phosphates in this inhibitor complex are fixed by interactions with a conserved glycine-rich loop and by ion pairing with Lys72. The phosphates are also secured by two Mg^{2+} ions. Since Mg^{2+} scatters weakly, it is often difficult to locate in macromolecular crystals. To overcome this problem, the crystals were soaked in Mn^{2+} which scatters more strongly and has a strong anomalous-scattering signal. This allows us to describe the metal binding sites in detail. In addition, the resolution of our structure was extended to 2.2 Å.

Experimental procedures. The wild-type mouse catalytic (C_α) subunit was expressed in *E. coli* and purified as described previously with some modification (Yonemoto, McGlone, Slice & Taylor, 1991). The protein contains several isoforms differing in degree of phosphorylation. After separation of the isoforms by Mono S chromatography (Herberg, Bell & Taylor, 1993), isoform II was selected for further crystallization. Isoform II contains three phosphates at Ser10, Thr197 and Ser338. The inhibitor peptide was synthesized by Advanced Chem. Tech. (Louisville, USA) and purified to homogeneity by high-performance liquid chromatography. The peptide constitutes the major inhibitory segment of PKI and has an apparent K_i of 2 n*M* (Cheng, van Patten, Smith & Walsh, 1986). The *C* subunit was crystallized as a ternary complex, using enzyme:inhibitor:Mg^{2+}:ATP molar ratios of 1:3:5:20. Crystals of the recombinant mouse *C* subunit complexed with MgATP and PKI(5-24) were grown according to Zheng, Knighton, Parello, Taylor & Sowadski (1991) and Zheng *et al.* (1993). One important modification of those conditions was the use of 0.4% (*w*/*v*) octanoyl-*N*-methylglucamide (MEGA-8) in the hanging drop.

* Current address for DRK: Agouron Pharmaceuticals Inc., 3565 General Atomics Court, San Diego, CA 92121, USA.

† To whom all correspondence should be addressed.

0907-4449/93/030362-04$06.00

The ternary complex crystallizes in space group $P2_12_12_1$ with unit-cell dimensions a = 73.58 , b = 76.28 and c = 80.58 Å. A crystal grown under conditions of low [Mg^{2+}] (0.44 m*M*) relative to ATP was soaked for 20 h in a 1 ml solution consisting of 17 m*M* bicine buffer pH = 8.0, 15% (*v*/*v*) MeOH, 2.7% (*w*/*v*) polyethylene glycol 400 (Dow), 1.66 m*M* ATP and 4.4 m*M* $MnCl_2$. Soaking did not result in any significant changes in the unit-cell dimensions of the crystal, which diffracted to 2.2 Å resolution.

Diffraction data were collected at 277 K with graphite-monochromated Cu $K\alpha$ X-rays from a Rigaku RU-200 rotating-anode diffractometer at the UCSD Research Resource equipped with two Xuong-Hamlin multiwire area detectors (Hamlin *et al.*, 1981; Xuong, Sullivan, Nielsen & Hamlin, 1985). Data reduction was performed using UCSD area-detector processing programs (Howard, Nielson & Xuong, 1985). Diffraction data were collected from one crystal, resulting in 21 443 (90.6% complete) reflections with R_{sym} = 6.9% ($R_{sym} = \Sigma|I_{obs} - I_{avg}|/\Sigma I_{avg}$) for all of the data and 7.9% for the shell between 2.37 and 2.20 Å. The model was refined with *X-PLOR* (Brünger, Kuriyan & Karplus, 1987) starting with phases from the refined 2.7 Å MgATP ternary complex (Zheng *et al.*, 1993).

Refinement was carried out using simulated-annealing (SA) and conjugate-gradient (CG) positional refinement with 15-2.2 Å data with $F > 2\sigma$ (17 868 reflections). ATP and Mg^{2+} were excluded from the starting model. Annealing from 2000 to 300 K brought the *R* factor to 24.9% using fixed B = 17 Å^2 for all atoms. To locate the ATP, a difference Fourier map was calculated at this point. Residues 49-60 and the peptide inhibitor (residues 361-380) were omitted from the phase calculation because of possible interactions with ATP. ATP built into this difference map adopts a very similar conformation to ATP reported earlier (Zheng *et al.*, 1993). Minor adjustment was made within the region containing residues 49-60 and 361-380 using the program *TOM/FRODO* (Cambillau & Horjales, 1987; Jones, 1978) and the resulting model, excluding ATP, was used to calculate an anomalous Fourier map using diffraction data from 10 to 4 Å. This map was essentially identical to the final anomalous Fourier map shown in Fig. 1. The two largest peaks clearly identify the positions of the two Mn^{2+} ions. Mn^{2+} and ATP were then included in the model, and CG refinement of this model resulted in R = 24.5%. At this stage, 53 water molecules were built in, based on difference maps in which only peaks higher than 3σ were considered. Inclusion of the 53 water molecules brought the *R* factor after CG refinement to 22.9%, still using a single B of 17 Å^2. Difference Fourier maps based on this model allowed an additional 40 water molecules to be built in using the same criteria, and their inclusion brought the *R* factor to 22.5% (again after CG refinement).

This model, refined with *X-PLOR* using restrained *B* factors, gave an *R* factor of 19.9% for $F > 2\sigma$, with r.m.s. deviations from ideal bond lengths and angles of 0.020 Å and 3.78°, respectively. To check the overall stability of the model, it was independently refined using *TNT* (Tronrud, 1992; Tronrud, Ten Eyck & Matthews, 1987) with unrestrained *B* factors and using all observed data. The *TNT* refinement produced an *R* factor of 17.7% for $F > 2\sigma$ (19.9% for all observed data), with r.m.s. bond-length and angle errors of 0.013 Å and 2.2°. During the *TNT* refinement, 220 atoms hit the upper limit B = 100 Å^2. None of the 103 solvent molecules refined to the *B* upper limit. 185 atoms with high *B*'s are side-chain atoms and among them, 70 atoms belong to side chains that were truncated due to lack of density in the binary complexes (Knighton *et al.*, 1993). 35 main-chain atoms with high *B*'s are located within the C-terminal region of the enzyme (residues 300-339) and the C terminus of the inhibitor peptide (residue 380). The remainder of the main-chain atoms with high *B*'s are located in portions of the molecule that are exposed to solvent. The main-chain residues (51-55) reported in the binary structure to have high *B*'s (Knighton *et al.*, 1993) exhibit low *B* factors in this ternary structure which can be explained by the presence of bound MnATP interacting with the glycine-rich loop. Only two residues (46 and 379) are not within allowed regions of the Ramachandran plot.

The r.m.s. difference between the C^{α} coordinates for the *TNT* and *X-PLOR* refinements was 0.21 Å, which is not significant at this resolution and *R* factor. The restrained *B*'s were much better behaved than the unrestrained *B*'s, but the latter are better indicators of reliability. The average restrained *B* for the *X-PLOR* refinement was 16.2 Å^2. The *TNT* unrestrained average *B*, excluding the atoms which hit the upper limit, was 32.4 Å^2.

Results. An anomalous Fourier map (Fig. 1) using data from 10 to 4 Å resolution shows the two largest peaks at the general location of previously identified Mg^{2+} metal sites confirming the assignment reported earlier (Zheng *et al.*, 1993). A detailed geometry of the MnATP site is shown in Figs. 1 and 2. The largest peak corresponds to the major site which is coordinated by the O atoms of the β- and γ-phosphates of ATP and the invariant Asp184. The next largest peak corresponds to the minor site which is coordinated by the O atoms of the γ- and α-phosphates of ATP and two invariant residues, Asn171 and Asp184. Thus, a comparison of the high-Mg^{2+} 2.7 Å structure with the high-Mn^{2+} structure described here shows no significant differences.

The high-resolution structure reveals additional solvent molecules coordinating the metal sites. The major Mn^{2+} metal site is now coordinated by two solvent molecules, bringing the total number of ligands for this metal site to six. The minor Mn^{2+} metal site is coordinated now by one solvent molecule, and thus, five ligands to this site are now visible. The invariant Asp184 in this inhibited structure serves as a ligand to both metal sites. The intermetallic distance, as calculated from the refined model, is 4.0 Å.

The invariant Asp166, proposed to be the general base for catalysis (Zheng *et al.*, 1993), is still close to the P site in the peptide, but now is also within the major hydrogen-bonding distance (2.5 Å) to one of the solvent molecules coordinating the major Mn^{2+} site.

Discussion. While the medium-resolution (2.7 Å) structure of the ternary complex of the catalytic subunit clearly identified the residues that specifically interact with MgATP and defined the unique features of the protein-kinase nucleotide fold, the precise geometry around the metal binding sites was less clear (Zheng *et al.*, 1993). In the medium-resolution (2.7 Å) crystals that were grown in low Mg^{2+}, density was seen clearly for only one site (Zheng *et al.*, 1993). Since one Mg^{2+} ion is required for nucleotide binding and catalysis (Armstrong, Kondo, Granot, Kaiser & Mildvan, 1979), we conclude that this corresponds to the major Mg^{2+} site that bridges the β- and γ-phosphates. A second site is only seen clearly when the metal-ion concentration is high. In terms of catalysis, binding of one Mg^{2+} ion is required while a second Mg^{2+} results in a 40–70% inhibition of activity (Armstrong *et al.*, 1979). The inhibitory effect of Mg^{2+} is most likely due to a tighter binding of ADP, since the release of ADP is the rate-limiting step in the reaction (Adams & Taylor, 1992; Kong & Cook, 1988). Mn^{2+} is qualitatively similar to Mg^{2+}; however, it binds more tightly and is a much more potent inhibitor (Armstrong *et al.*, 1979; Bhatnagar, Roskoski, Rosendahl & Leonard, 1983). Although this structure represents an inhibitor complex, previous NMR studies using substitution-inert complexes of ATP

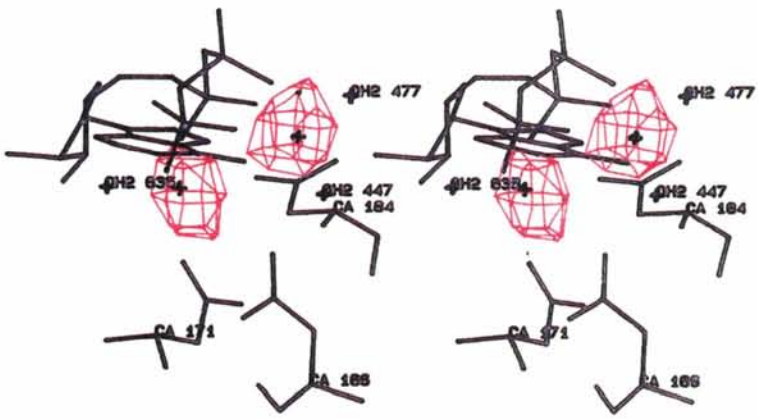

Fig. 1. Stereoview of an anomalous Fourier map superimposed with the MnATP binding-site region. This map was calculated using the final refined set of phases and diffraction data from 10–4 Å resolution (6338 unmerged reflections used here account for 80% of all possible Bijvoet reflection pairs in this resolution range). The map was contoured at 3.5σ. The two highest peaks (4.6 and 4.3σ) correspond to two Mn^{2+} metal ions. The first noise peak (4.1σ) is located at the main-chain position of residue 36. Two Mn^{2+} metal ions, shown as black crosses and located in the centers of the two peaks, are 4.0 Å apart. The primary metal site O*M*382 is coordinated by the O atoms of the γ- (2.1 Å) and β-phosphate (2.2 Å), by the invariant Asp184, which provides two ligands (2.4 and 2.2 Å), and by two water molecules, $OH_2$477 (1.9 Å) and $OH_2$447 (2.2 Å). The secondary metal site, O*M*383, is coordinated by the O atoms of the γ- (2.2 Å) and α-phosphate (2.0 Å), by the invariant Asn171 (2.1 Å), by Asp184 (2.1 Å), and by one water molecule, $OH_2$635 (2.1 Å).

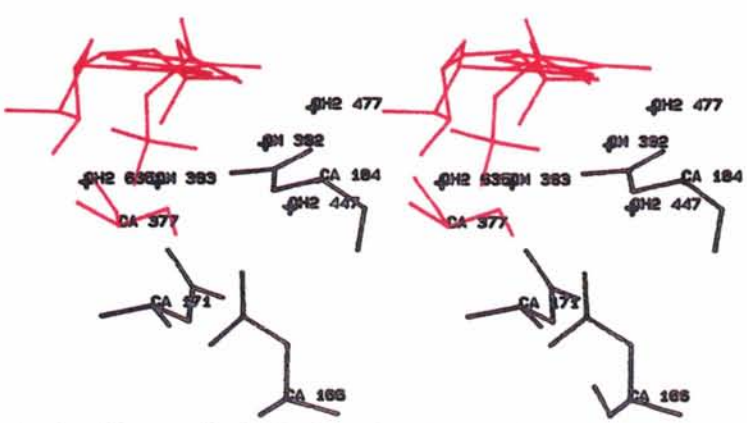

Fig. 2. Environment of conserved amino acids surrounding the site of phosphotransfer. For this diagram, a serine (shown in red) was modeled into the P site so that distances between the γ-phosphate and a protein substrate could be estimated. The primary metal site, O*M*382, is coordinated by the invariant Asp184, as well as two water molecules as indicated above. The secondary inhibitory metal site, O*M*383, is coordinated by the invariant Asn171, by invariant Asp184, as well as by one water molecule. Asp184, therefore, is shared by both metal sites in this inhibited complex.

such as $Co^{3+}(NH_3)_4$AMPPCP, also indicated that the first metal binding site bridging the γ- and β-phosphates is activating while the second metal binding site, seen here as bridging the γ- and α-phosphates, is inhibitory, and this is consistent with our observations (Granot, Mildvan, Bramson & Kaiser, 1980).

While the distance between metals differs slightly from those observed using NMR (4.8 Å based on NMR *versus* 4.0 Å based on the 2.2 Å crystal structure), the general location of the metals is consistent with those earlier results (Granot *et al.*, 1980). According to the NMR results, the secondary metal site was predicted to interact tightly with protein side chains, while the primary metal bridging the β- and γ-phosphates did not interact with protein. This is inconsistent with the interactions of Asp184 with the primary metal site seen here. This discrepancy may be due to the fact that the NMR studies used a substitution-inert ATP analog which could distort interactions with the β- and γ-phosphates. The fact that the Mn^{2+} structure represents an inhibitor complex where both peptide and ATP are binding with a high affinity (2.0 and 60 n*M*, respectively) may also be significant (Cheng *et al.*, 1986; Whitehouse & Walsh, 1983). The P site in this inhibitor complex is occupied by an alanine. By modeling a serine into this position one can begin to understand the general relationship of substrate, the γ-phosphate of ATP, and conserved residues at the active site (Fig. 2). The Ser-OH is less than 3 Å from the side chain of Asp166, predicted to serve as a catalytic base, and is also less than 3 Å from the γ-phosphate. Asp166 in this inhibitor complex also interacts with one of the water molecules, $OH_2$447, that coordinates the primary metal site. This location of conserved residues adjacent to the reaction pathway is consistent with the direct in-line transfer mechanism predicted by Ho, Bramson, Hansen, Knowles & Kaiser (1988) with the formation of a pentacovalent intermediate.

This work was supported by the Lucille P. Markey Charitable Trust, by grants from NIH (SST, N-hX and JMS), NSF (SST and LFTE), and NIH training grants T32CA09523 and T32DK07233 (DRK). We thank the following individuals and resources for their contributions: Gene Hasegawa for help in preparation of this manuscript; Sean Bell for technical assistance; the NIH National Research Resource at UCSD (RR01644) and staff members Chris Nielsen and Don Sullivan for data-collection facilities; the San Diego Supercomputer Center for use of the Advanced Scientific Visualization Laboratory and the Cray Y-MP8/864.

The coordinates for the binary complex are available from the Brookhaven Protein Data Bank as entry 2CPK. The coordinates and structure factors of this ternary complex have been deposited with the Brookhaven Protein Data Bank.*

* Atomic coordinates and structure factors have been deposited with the Protein Data Bank, Brookhaven National Laboratory (Reference: 1ATP, R1ATPSF). Free copies may be obtained through The Technical Editor, International Union of Crystallography, 5 Abbey Square, Chester CH1 2HU, England (Supplementary Publication No. SUP 37078). At the request of the authors, the structure factors will remain privileged until 1 April 1994. A list of deposited data is given at the end of this issue.

References

ADAMS, J. A. & TAYLOR, S. S. (1992). *Biochemistry*, **31**, 8516-8522.
ARMSTRONG, R. N., KONDO, H., GRANOT, J., KAISER, E. T. & MILDVAN, A. S. (1979). *Biochemistry*, **18**, 1230-1238.
BHATNAGAR, D., ROSKOSKI, R. J., ROSENDAHL, M. S. & LEONARD, N. J. (1983). *Biochemistry*, **22**, 6310-6317.
BRÜNGER, A. T., KURIYAN, J. & KARPLUS, M. (1987). *Science*, **235**, 458-460.
CAMBILLAU, C. & HORJALES, E. (1987). *J. Mol. Graphics*, **5**, 174.
CHENG, H.-C., VAN PATTEN, S. M., SMITH, A. J. & WALSH, D. A. (1986). *Biochem. J.* **231**, 655-661.
GRANOT, J., MILDVAN, A. S., BRAMSON, H. N. & KAISER, E. T. (1980). *Biochemistry*, **19**, 3537-3543.
HAMLIN, R., CORK, C., NIELSEN, C., VERNON, W., MATTHEWS, D., XUONG, N. & PEREZ-MENDEZ, V. (1981). *J. Appl. Cryst.* **14**, 85-93.
HANKS, S. K., QUINN, A. M. & HUNTER, T. (1988). *Science*, **241**, 42-52.
HERBERG, F. W., BELL, S. & TAYLOR, S. S. (1993). *J. Biol. Chem.* Submitted.
HO, M.-F., BRAMSON, H. N., HANSEN, D. E., KNOWLES, J. R. & KAISER, E. T. (1988). *J. Am. Chem. Soc.* **110**, 2680-2681.
HOWARD, A. J., NIELSON, C. & XUONG, N. (1985). *Methods Enzymol.* **14**, 452-472.
JONES, T. A. (1978). *J. Appl. Cryst.* **11**, 268-272.
KNIGHTON, D. R., BELL, S. M., ZHENG, J., TEN EYCK, L. F., XUONG, N., TAYLOR, S. S. & SOWADSKI, J. M. (1993). *Acta Cryst.* D**49**, 357-361.
KNIGHTON, D. R., ZHENG, J., TEN EYCK, L. F., ASHFORD, V. A., XUONG, N., TAYLOR, S. S. & SOWADSKI, J. M. (1991). *Science*, **253**, 407-414.
KONG, C.-T. & COOK, P. F. (1988). *Biochemistry*, **27**, 4795-4799.
TRONRUD, D. E. (1992). *Acta Cryst.* A**48**, 912-916.
TRONRUD, D. E., TEN EYCK, L. F. & MATTHEWS, B. W. (1987). *Acta Cryst.* A**43**, 489-501.
WHITEHOUSE, S. & WALSH, D. A. (1983). *J. Biol. Chem.* **258**, 3682-3692.
XUONG, N., SULLIVAN, D., NIELSEN, C. & HAMLIN, R. (1985). *Acta Cryst.* B**41**, 267-269.
YONEMOTO, W., MCGLONE, M. L., SLICE, L. W. & TAYLOR, S. S. (1991). *Protein Phosphorylation*, Part A, edited by T. HUNTER & B. M. SEFTON, pp. 581-596. San Diego: Academic Press.
ZHENG, J., KNIGHTON, D. R., PARELLO, J., TAYLOR, S. S. & SOWADSKI, J. M. (1991). *Protein Phosphorylation*, Part A, edited by T. HUNTER & B. M. SEFTON, pp. 508-521. San Diego: Academic Press.
ZHENG, J., KNIGHTON, D. R., TEN EYCK, L. F., KARLSSON, R., XUONG, N., TAYLOR, S. S. & SOWADSKI, J. M. (1993). *Biochemistry*. In the press.